Polymer Chemistry

PAPER

View Article Online
View Journal | View Issue

Cite this: *Polym. Chem.*, 2016, **7**, 6752

Click reactive microgels as a strategy towards chemically injectable hydrogels†

Rémi Absil,[a,b,c,d] Seda Çakir,[b] Sylvain Gabriele,[e] Philippe Dubois,[a] Christopher Barner-Kowollik,*[c,d] Filip Du Prez*[b] and Laetitia Mespouille*[a]

Received 23rd September 2016,
Accepted 12th October 2016

DOI: 10.1039/c6py01663d

www.rsc.org/polymers

Doubly crosslinked microgels (DX microgels) are hydrogels constructed by covalently interlinked microgel particles, offering two levels of hierarchy within the network, the first one being the microgel and the second being the interlinked microgel network. Herein we describe an efficient approach for DX microgel synthesis *via* the ultrafast triazolinedione (TAD)-based click reaction. Cyclopentadienyl functional microgels were prepared by a conventional water in oil (W/O) suspension, free-radical copolymerization of poly(ethylene glycol)methyl ether methacrylate (M_n = 500 g mol^{-1}) with glycidyl methacrylate and ethylene glycol dimethacrylate as crosslinkers. Microgel post-modification was subsequently achieved by reacting glycidyl functions with sodium cyclopentadienide (NaCp), resulting in Cp-functionalized microgels. Finally, the microgels were mixed with a bis-TAD functional crosslinker, resulting in crosslinking with adequate kinetics (minutes to seconds) to form a doubly crosslinked microgel network. Size distributions of swollen microgels before creation of the second network were followed by optical microscopy and particle size measurements. The efficient functionalization of the microgels with Cp units was demonstrated by a fluorescence labelling study. Dynamic rheology data showed the increase of mechanical properties from the microgels to the doubly crosslinked microgel network formed after addition of the TAD crosslinker. The current study thus highlights the efficiency of catalyst free modular ligation chemistry to synthesize DX microgels with a very fast gelation process from 5 minutes to 15 seconds depending on the crosslinker to Cp ratio, from 0.7 to 1 respectively.

Introduction

The rise in the number of serious illnesses reported in the world's population, together with the need to provide better healthcare solutions has pushed the research community to develop more creative and efficient materials that could improve treatments. Among the various strategies reported in the literature, *in situ* forming hydrogels, also called injectable hydrogels, are gaining an increasing deal of interest over the past few years owing to their ability to deliver locally and in a minimally invasive manner therapeutics or living cells upon direct injection. *In situ* forming hydrogels are polymer materials that spontaneously gelate under physiological conditions to form three-dimensional structures, and with the potential to take place into sites that are not accessible surgically. Furthermore, injectable hydrogels can easily adapt their shape to a complex geometry and can adhere to the surrounding tissues during hydrogel formation, without altering the natural tissue structure.[1,2] More interestingly, gelation can occur in the presence of therapeutics (drugs, bioactive molecules or cells), leading to a drug delivery device with controlled release profile at the site of application, overcoming biological obstacles and, in particular cases, the dose-limiting toxicity.[2,3] From a polymer chemistry viewpoint, polymeric materials should meet specific criteria to be used for *in situ* forming hydrogel applications such as adequate viscosity allowing an easy injection, a fast transition from liquid/viscous solution of polymer precursors to a solid, biocompatibility and appropriate physical and mechanical properties for the targeted appli-

[a]*Laboratory of Polymeric and Composite Materials (LPCM), Center of Innovation and Research in Materials and Polymers (CIRMAP), Health and Materials Research Institutes, University of Mons (UMons), 23 Place du Parc, 7000 Mons, Belgium. E-mail: Laetitia.mespouille@Umons.ac.be; Fax: +326537348; Tel: +3265373482*
[b]*Polymer Chemistry Research Group, Ghent University, Krijgslaan 281 S4-bis, B-9000 Ghent, Belgium. E-mail: Filip.DuPrez@Ugent.be; Fax: +3292644972; Tel: +3292644503*
[c]*Preparative Macromolecular Chemistry, Institut für Technische Chemie und Polymerchemie, Karlsruhe Institute of Technology (KIT), Engesserstr. 18, 76128 Karlsruhe, Germany*
[d]*Institut für Biologische Grenzflächen, Karlsruhe Institute of Technology (KIT), Hermann-von-Helmholtz-Platz 1, 76344 Eggenstein-Leopoldshafen, Germany. E-mail: christopher.barner-kowollik@kit.edu; Fax: +4972160845740; Tel: +4972160845641*
[e]*Laboratoire Interfaces & Fluides complexes, CIRMAP, Research Institute for Biosciences, University of Mons, 23 Place du Parc, 7000 Mons, Belgium*
†Electronic supplementary information (ESI) available. See DOI: 10.1039/c6py01663d

cation.[4] Injectable hydrogels can be divided into two categories according to their gelation process: chemically crosslinked or physically crosslinked. The latter arises from secondary, weak interactions such as electrostatic interactions,[5–9] host guest interactions,[10–14] stereo-complexation[15–17] or sol–gel transition induced by subtle changes under environmental conditions.[18–20] Physical hydrogels offer a gentle gelation process, limiting the denaturation of incorporated drug/proteins and damage embedded cells and surrounding tissues. While less attractive in their infancy, chemically crosslinked injectable hydrogels are also gaining interest. They are usually prepared by UV irradiation[21–24] or covalent bonding[25–27] and they undergo a large volume change during the transition phase.

Major attention has been devoted to understand the relationship between sophisticated structures and properties in order to open up and design the range of applications of injectable hydrogels. In this context, doubly crosslinked (DX) microgels are a new class of injectable hydrogels that bring two levels of structural hierarchy.[28–32] Indeed, DX microgels that consist of internally crosslinked particles (micro- or nano-sized gels) are able to establish connections with their partners through an inter-crosslinking process. Unique properties such as fine tuning of mechanical properties, DX microgel mesh size, high specific surface area, controlled heterogeneity at the nanoscale as well as moldable hydrogels that flow on applied stress are all benefits that can emerge from this network construction.[29,33] The first paper describing DX microgels was published in 2000 by Hu *et al*.[34] In their report, they described the synthesis of a new class of nanostructured polymer gels by bonding crosslinked hydroxypropyl cellulose nanoparticles with divinyl sulfone in solution at 55 °C. This increasing level of structural complexity offers great promise for regenerative medicine also in which injectable DX microgels have been investigated for degenerative intervertebral disc treatment,[35] vocal fold restoration[29] or mesenchymal stem cell differentiation.[30] Owing to the existence of two levels of cross-linking, degradation and mechanical properties of the resulting hydrogel can be adjusted independently and therefore the responsivity of the materials increases greatly.

Various different strategies to synthesize DX microgels have been published so far. Mostly, they are obtained by covalent coupling *via* a free-radical polymerization process of pending vinyl bonds localized at the particle surfaces.[30,33,35–44] Only a few examples report physical inter-crosslinking[45,46] whilst still being efficient enough to produce hierarchized injectable networks embedding micro- to nanoparticles. The heat released during the polymerization process and/or polymerization conditions (temperature higher than body temperature) are not always compatible with *in vivo* prerequisites. As a consequence, covalent coupling reactions that occur fast and at room temperature are really desirable. The realm of click chemistry reactions offers a large choice for fast coupling reaction at room temperature.[47–51] However, while being a valuable tool for many coupling reactions, this family of reactions has never been investigated so far in DX microgel formation, except to introduce vinyl functions onto microparticle surfaces as reported recently by Saunders *et al.* In their strategy, copper catalyzed azide–alkyne cycloaddition (CuAAC) was investigated to precisely control the extent of vinyl functionalization of the microgel (MG) particles and therefore dial up the modulus of the resulting DX microgels.[52]

Herein, we describe for the first time the use of a metal-free, click coupling reaction to interlink well-defined microparticles. In particular, we are taking advantage of the 1,2,4-triazoline-3,5-dione (TAD) based click chemistry, as previously introduced by some of us.[53–55] TAD chemistry is a promising approach as it displays an extremely high reactivity towards enes and dienes, favoring ultrafast Diels–Alder and ene-type reactions. Typically, these reactions occur in a time scale of seconds at room temperature with high conversion and without the need of any catalyst or stimuli. More interestingly, the reddish color of the TAD compound disappears after ene-coupling resulting in a colorless product, offering a visual feedback of the progress of the reaction.[56] According to these outstanding properties, it is believed that the TAD-based coupling reaction may provide an advantageous tool to prepare DX microgels with an easy setup, a fast processability at r.t., injectability and variation of the DX microgel modulus. In this study, our approach is based upon the synthesis of polyethylene glycol (PEG)-based microgels obtained by water in oil (W/O) conventional suspension free-radical copolymerization of poly(ethylene glycol)methyl ether methacrylate (PEGMA, M_n: 500 g mol^{-1}) with a glycidyl methacrylate (GMA) and ethylene glycol dimethacrylate (EGDMA) crosslinker followed by the derivatization of glycidyl groups with cyclopentadienyl (Cp) compounds. DX microgels were then obtained in a catalyst and initiator-free approach by mixing the Cp-functionalized microparticles in the presence of a bis-TAD crosslinker (Fig. 1). The ultrafast kinetic reaction of TAD with Cp allowed for the formation of DX microgels within a time-frame of seconds. Optical microscopy and particle size measurements were used to probe the size and morphologies of the microgels. Fluorescence microscopy investigations demonstrated the

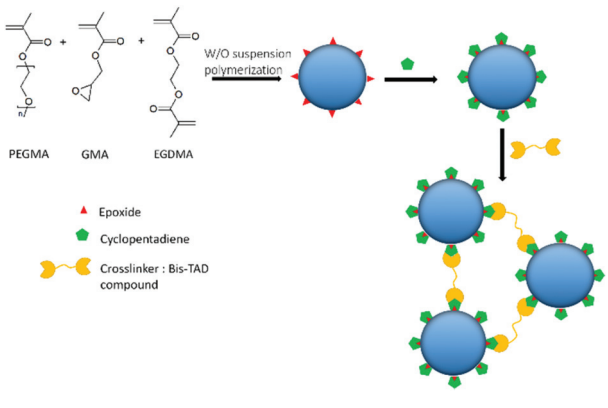

Fig. 1 Illustration of the synthetic steps for the design of doubly crosslinked injectable microgels *via* click chemistry between cyclopentadiene and triazolinedione groups.

grafting and qualitatively quantified the efficient graft of cyclopentadiene onto the surface of the microgels while UV measurements gave information about quantitative surface Cp functionality. Mechanical properties of the microgel suspensions and the resulting DX microgels were investigated by rheology.

Results and discussion

Cyclopentadienyl functional microgels

In the strategy investigated here, doubly crosslinked (DX) network preparation *via* the Hetero Diels–Alder (HDA) reaction firstly requires the synthesis of microgels, equipped with clickable groups. The highly reactive cyclopentadiene (Cp) was chosen as the diene of choice to decorate the microgels since Cp is one of the most reactive dienes for Hetero-Diels Alder (HDA) reactions.[57] The Cp-functionalized microgels were synthesized according to a protocol inspired by the work of the Barner-Kowollik team.[58] In their work, porous glycidyl-based microspheres were produced by suspension polymerization followed by a post-modification reaction with sodium cyclopentadienide. In this context, the glycidyl moiety represents an advantageous function for post-modification reactions as the epoxide group can react in many ways.[59]

Here, a series of glycidyl-based microgels were prepared by water-in-oil (W/O) suspension free-radical copolymerization of glycidyl methacrylate (GMA), poly(ethylene glycol)methyl ether methacrylate (PEGMA) and ethylene glycol dimethacrylate (EGDMA). The free-radical polymerization was conducted in water droplets dispersed in cyclohexane under strong stirring with an initial monomer concentration of 40%. The polymerization was initiated at 70 °C using 4,4′-azobis(4-cyanovaleric acid) as a free-radical precursor. Small-sized and non-aggregated microparticles were achieved by using a mixture of SPAN 80/TWEEN 80 (5.6/1 molar ratio) surfactants that guarantee stable droplet formation and afterwards, non-aggregated microgels with narrow size distribution were achieved. The initial co-monomer molar ratio $[GMA]_0/[PEGMA]_0/[EGDMA]_0$ was fixed to 3/7/1 and 3/7/1.5, which led to a molar composition in a glycidyl function of 28.1% and 26.8%, respectively. In the first series of experiments, the impact of the stirring rate on the particle size was studied by applying stirring rates of 1200, 800, 400 and 200 rpm. Similarly, the impact of the crosslinker density in microgels was also varied. The polymerizations were stopped after 6 h of reaction and the resulting microgels were purified by extensive washing in ethanol to get rid of any soluble fractions and surfactants. Size and size distribution were investigated by particle size measurements. The morphology of PEG microgels was also characterized by optical microscopy (Fig. 2). Table 1 shows the evolution of the microgel diameter as a function of the stirring rate and the crosslinker density. First of all, optical microscopy confirmed the formation of well-defined rounded microgels as well as the stability of the starting droplets (see the ESI S1†).

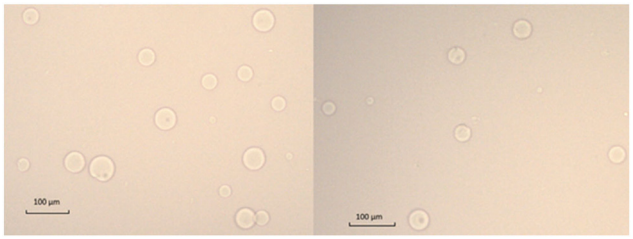

Fig. 2 Images of the purified glycidyl-based microgels (entry C, Table 1) obtained by optical microscopy in deionized water at r.t. before (left) and after functionalization by NaCp.

Table 1 Evolution of microgel size depending on the stirring rate and crosslinker density

Sample	$[M]_0/[I]_0/[C]_0$ [a]	Stirring rate (rpm)	Size[b] (µm)
A	1/0.05/0.1	1200	12 ± 2.5
B	1/0.05/0.1	800	22 ± 5.2
C	1/0.05/0.1	400	40 ± 12.6
D	1/0.05/0.1	200	90 ± 40
E	1/0.05/0.15	200	65 ± 25

[a] $[M]_0/[I]_0/[C]_0$: initial monomer/initiator/crosslinker molar ratio. [b] Size and size distribution as measured by a particle sizer in water at r.t.

As expected, increasing the stirring rate led to smaller microgels, ranging from 90 µm (200 rpm) to 22 µm (800 rpm). In addition, a small increase in the crosslinker molar composition led to a significant decrease of the microgel size. More importantly, size and size distribution measured by both techniques were in good agreement.

In the second step, reactive cyclopentadienyl groups were installed on microgels through nucleophilic addition onto the ring-strained epoxide. Practically, the GMA based-microgels were functionalized in a single step by suspending the microgels in anhydrous THF and subsequently adding a solution of sodium cyclopentadienide (Fig. 4). The cyclopentadienide anion reacts rapidly, following a nucleophilic addition onto the epoxide ring. After only 1 h at 0 °C and 3 h at r.t., the reaction was quenched with a saturated solution of ammonium chloride and the amber-like particles were purified by filtration followed by extensive washing with a saturated aqueous solution of ammonium chloride, acetone, water, acidic water (3% HCl), ethanol/water (1/1), tetrahydrofuran and ethanol to isolate the Cp-functionalized microgels (Table 2). Interestingly,

Table 2 Evolution of the microgel size after functionalization by sodium cyclopentadienide

Sample	Size before derivatization[a] (µm)	Size after Cp derivatization[a] (µm)
A	12 ± 2.5	12 ± 2.5
B	22 ± 5.2	23 ± 5.2
C	40 ± 12.6	41 ± 12.6

[a] Size and size distribution as measured by a particle sizer in water at r. t.

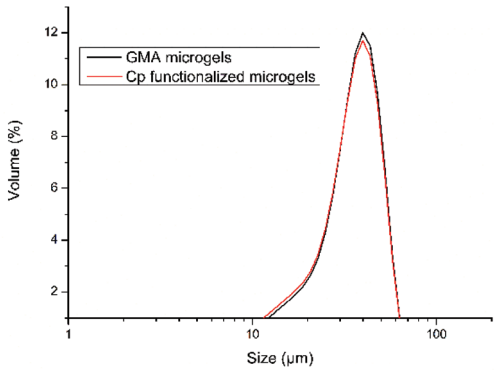

Fig. 3 Particle size distribution as measured by a particle sizer before (black) and after (orange) derivatization by sodium cyclopentadiene (microgels from entry C, Table 1).

no change in size and size distribution was noticed after Cp derivatization, as depicted in Fig. 2 and 3.

Beyond the change of coloration of the microparticle batch after treatment with NaCp, the success of the derivatization can be attested indirectly by fluorescence microscopy. For this purpose, Cp-functionalized microgels were reacted with the fluorescent marker *N*-(1-pyrene)maleimide (Pyr-Mal) *via* the Diels–Alder reaction at 40 °C for 3 hours (Fig. 4). As depicted in Fig. 5, microgels show fluorescent activity upon irradiation with UV light (366 nm), demonstrating the grafting of pyrene onto the surface of the particles. Moreover, surface functionalization was attested by fluorescence microscopy as shown in Fig. 5b and c. Both analyses demonstrate unambiguously that microgels were well derivatized with Cp and that Cp surface distribution is homogeneous on a micrometer scale. As a control, glycidyl-based microgels subjected to the same washing steps as their Cp-functionalized counterparts did not show any fluorescence.

Controlling the kinetics of DX microgel formation is an important issue that needs to be addressed depending on the targeted application. It can be anticipated that the density of reactive dienes onto the surface will strongly influence the rate of gelation. Herein, tuning Cp density onto the surface is an interesting strategy to set up the kinetic window of gelation. For this purpose, GMA-based microgels were subjected to a post-modification reaction with various quantities of NaCp solution. Cp density modulation and distribution on the microgel can be followed qualitatively by indirect measure-

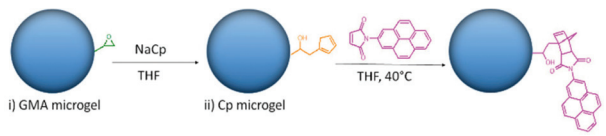

Fig. 4 Schematic overview of the functionalization and grafting reactions on microgels. (i) GMA functionalized microgels are functionalized with Cp by the reaction with sodium cyclopentadienide solution in anhydrous THF. (ii) The Cp-functionalized microgels undergo Diels–Alder reactions with the fluorescent marker *N*-(1-pyrene)maleimide.

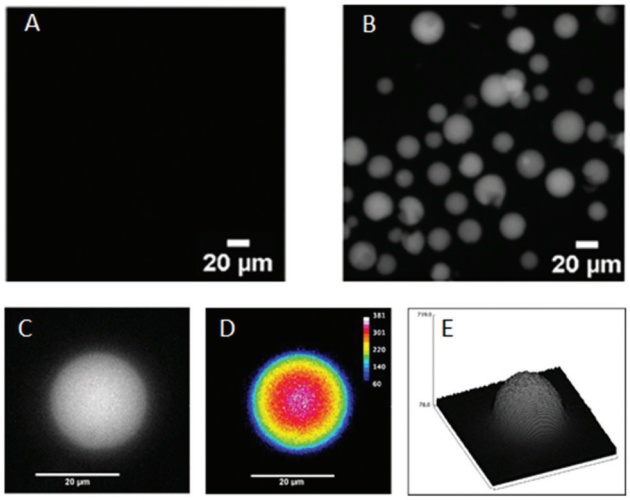

Fig. 5 Fluorescence analysis of (A) Cp microgels (negative control), (B) fluorescence image of microgels after *N*-(pyrene)maleimide functionalization, (C) high magnification image of a microgel after *N*-(pyrene)maleimide functionalization, (D) color-coded fluorescence image with *N*-(1-pyrene)maleimide and (E) surface plot representation of the fluorescence on a microgel surface (reconstructed from (D)).

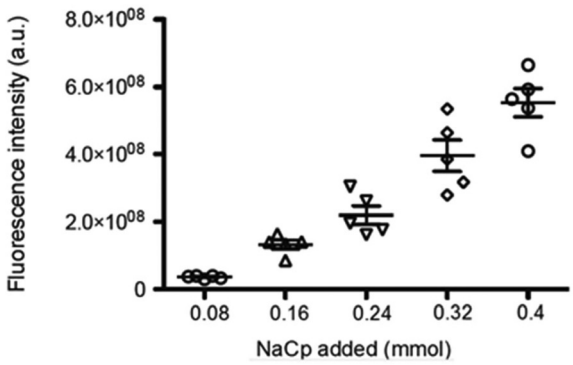

Fig. 6 Linear increase of the fluorescence intensity of the Pyr-based microgels in direct correlation with the quantity of the NaCp derivatizing agent.

ments of fluorescence microscopy after derivatization of Cp with *N*-(1-pyrene)maleimide. Indeed, with this DA click reaction being quantitative and fast, it can be assumed that the fluorescence intensity of pyrene can be directly correlated with the Cp quantity. For this study, a microgel sample was derivatized with a quantity from 0.08 to 0.4 mmol of NaCp and finally by pyrene-maleimide.

As depicted in Fig. 6, a linear increase of the fluorescence of the beads as a function of mmol of the NaCp derivatizing agent is reported, with a reasonable regression coefficient. This study confirms that we can control the density functionalization of the microgels with a good level of reproducibility, which paves the way towards the on-demand gelation kinetics of DX microgel formation. Qualitatively speaking, fluorescence measurements prove the effective grafting of Cp func-

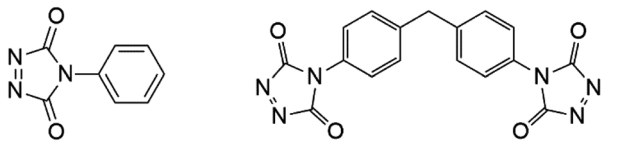

Fig. 7 Structure of 4-phenyl-1,2,4-triazoline-3,5-dione (PTAD) (left) and 4,4′-(4,4′-diphenylmethylene)-bis-(1,2,4-triazoline-3,5-dione) (MDI-TAD) (right).

tions onto the surface, their homogeneous distribution and their reactivity.

Fast inter-crosslinking and a high degree of gelation being prerequisites to some bio-related applications, quantitative estimation of the amount of Cp available on the surface is of upmost importance in order to be able to determine the quantity of crosslinker that should be added to the medium. Quantification of Cp functions was further approached by titration of Cp moieties using an UV sensitive reactant that could react instantaneously and quantitatively with the diene. For this study we took advantage of the recently developed triazolinedione TAD click chemistry (colour switch), which fits perfectly with the titration prerequisite and offers more accurate values of the Cp content than fluorescence measurements. The reaction was performed on two sets of particles, the size of which is centered around 12 ± 2.5 and 41 ± 12.6 μm (Table 1, entries A and C) with available 4-phenyl-1,2,4-triazoline-3,5-dione (PTAD) (Fig. 7, left) as a simple UV-sensitive titration molecule at room temperature in butyl acetate. An excess of PTAD arising after saturation of the Cp-based microgels was measured by UV and quantified by means of a calibration curve (A = 148.49, λ = 540 nm, see the ESI†). Therefore, the Cp content was indirectly determined *via* quantification of the PTAD amount remaining in solution.

As expected for an equal quantity of starting microgels, smaller particles require more PTAD solution to saturate the microgel surfaces as a result of their higher specific surface area. Therefore, it was calculated that 137 nmol *versus* 66 nmol of Cp were required to saturate 80 mg of 41 μm and 12 μm size particles, respectively.

Synthesis of doubly crosslinked microgel (DX microgel) by TAD click chemistry

Doubly crosslinked (DX) microgels arise from covalent bonding between microgels, resulting in a permanent monolithic hydrogel. An efficient conjugation process is therefore required to link soft microbeads all together. In the field of this work where beads are in the size range of microns, it is of importance to select a conjugation process that ensures the coupling of localized functions in an additive-free way. Hetero Diels Alder click reactions involving Cp have already been demonstrated as a powerful technique in terms of efficiency, allowing us to obtain very high molecular weight block copolymers in less than 10 minutes, starting from end-functional, high molecular weight, polymer precursors.[60,61] Herein, we take advantage of the ultrafast TAD-based HDA click chemistry to interconnect the microgels. For this purpose, a bis-TAD functional crosslinker, 4,4′-(4,4′-diphenylmethylene)-bis-(1,2,4-triazoline-3,5-dione) (MDI-TAD, Fig. 6 right), was synthesized according to a reported procedure.[53]

Practically, a concentrated suspension of microgels was stirred at r.t. and MDI-TAD was added directly into the suspension. Different amounts of crosslinkers were added, based on the Cp content as titrated by UV, to check the influence of the crosslinker quantity on the gel formation. Hydrogel formation begins immediately after addition of the MDI-TAD. At too low MDI-TAD concentration, there is insufficient amount of the crosslinker and a homogeneous hydrogel cannot be obtained. On the other hand, when too high concentrations of MDI-TAD were used, gelation did not occur. Obviously, the first HDA reaction is faster than the second reaction step, which results in saturation of the Cp moieties at higher crosslinker concentrations. Only at intermediate MDI-TAD concentrations, homogeneous hydrogels were formed within seconds, as shown in Fig. 8 and Table 3.

Dynamic rheology was used to probe the mechanical properties of the DX microgels using parallel plate geometry. The data was compared to the precursor microgel suspension in the swollen state. The microgel suspension was homogeneously dispersed before DX microgel formation to promote homogeneous density of the microgel in the resulting DX microgel. The storage modulus, G', reflects the solid-like component of the rheological behavior, which is thus low at solution stage but increases drastically after gelation (G'' is the loss modulus and $\tan\delta = G''/G'$). Samples are first subjected to a strain sweep from 0% to 15% to define the linear viscoelastic region in which the modulus G' and G'' are independent of the applied strain. In our experiment, the strain amplitude was set as 0.5% and G' and G'' of the different DX microgels were probed over a period of measurements of 5 minutes duration to verify the influence of the crosslinker quantity on G' of the resulting DX microgel.

For both DX microgels and microgel suspension, the storage modulus (G') values are higher than the loss modulus indicating a gel-like behavior as defined in Winter and Chambon criteria.[62] This data shows that the precursor microgel suspension exists as physical gels prior to second crosslinking as also stated in the paper of Saunders *et al.*[63] The vari-

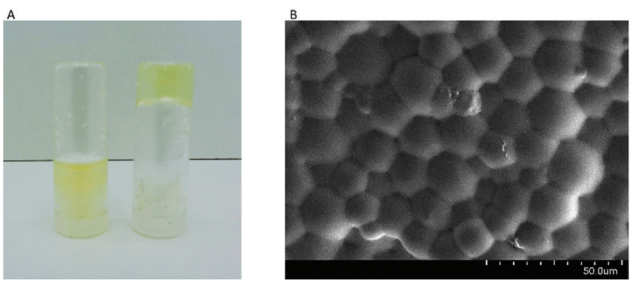

Fig. 8 (A) Picture of gel (right) formed within 2 minutes after addition of the MDI-TAD onto microgel suspension (entry D Table 3) and (left) microgel suspension (entry A Table 3). (B) SEM image of a DX gel.

Table 3 G' evolution of the DX microgels with the TAD/Cp ratio

Samples	Ratio TAD/Cp	Gelation time (s)	G' (Pa)
A	0	No gel	25
B	0.7	300	86
C	0.8	15	90
D	0.875	15	112
E	1.05	15	92
F	1.22	30	84
G	2.5	No gel	24

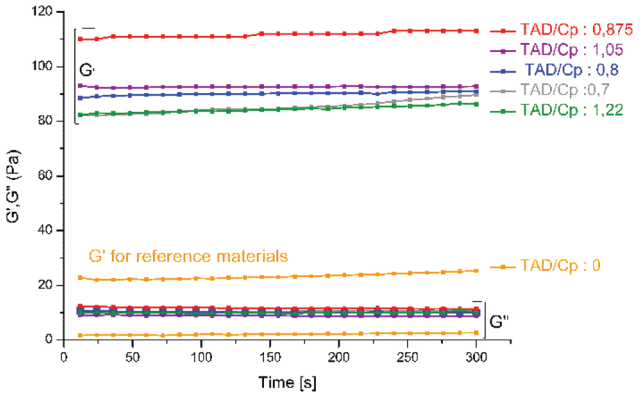

Fig. 9 Mechanical property characterization of DX microgels obtained at various TAD/Cp ratios and of the starting microgel suspension by rheology at r.t.

ation of G' for the DX micro-gels as a function of the cross-linker quantity is shown in Fig. 9.

This data reveals that the DX microgels had consistently higher G' values than the precursor microgel suspension (entry A) and that the G' value increased by approximately a factor of 4 for the DX microgel (see Table 3). The increased G' values can be attributed to the additional covalent crosslinking adduct from the cyclopentadiene/TAD reaction. It was expected that increasing the crosslinker quantity will lead to a higher value of G' but interestingly, a maximum in G' is observed after adding an amount of MDI-TAD, corresponding to a ratio of TAD/Cp of 0.875. Confirming previous observations, a further increase in the quantity of MDI-TAD leads to a decrease of the storage modulus and even to no gelation if a large amount of MDI-TAD is added as depicted in Fig. 10.

This decrease in G' and gelation time can be explained by saturation of the microgel surface by the MDI-TAD, decreasing the Cp content available to promote the formation of the second network. This data nicely validates our approach to prepare DX microgels by click chemistry.

Conclusions

We have investigated PEG-based, soft, hydrogel microspheres (microgels) and doubly crosslinked microgel networks (DX microgel) as injectable materials. Microgels with diameters

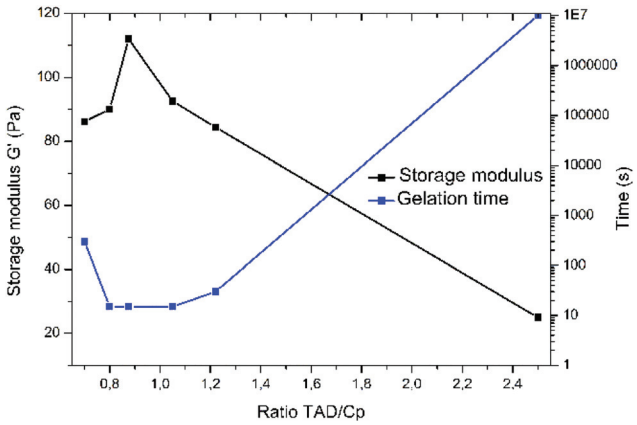

Fig. 10 Comparative evolution of G' (in black) and gelation time (in blue) with the TAD/Cp ratio.

from 12 to 90 μm were synthesized by water in oil suspension free-radical polymerization, followed by surface modification, to introduce very reactive functionalities onto the microgel surface with a tunable amount of clickable functions. The detailed analysis not only allowed for qualitative characterization but also for quantification of the Cp content on the microgel surface. Subsequent secondary crosslinking of the microgels with MDI-TAD resulted in macrogels with two levels of cross-linking, *i.e.* one within the individual microgels and the other one between the microgels. The click chemistry used to form the second crosslink works as a very efficient way to crosslink microgels and presents many advantages: easy handling, fast and no catalyst needed for the gelation reaction. The mechanical properties were probed by dynamic rheology. The storage modulus varied with the relative proportion crosslinker/microgel functionality and can be tuned depending on the crosslinker quantity with an improvement of a factor 4 for a relative ratio TAD/Cp of 0.875. Adapted mechanical property, biocompatibility and toxicity tests should be carried out for potential applications *in vivo*. Mechanical property tuning will be investigated in a forthcoming study by assessing the influence of different parameters such as the influence of direct pressure on the materials, multiple applied pressures, particle size, effect of mixing different particle sizes and crosslinking density on the microgel level.

Experimental

Materials

Polyethylene glycol methyl ether methacrylate (PEGMA, M_n: 500 g mol^{-1}), glycidyl methacrylate (97%) and ethylene glycol dimethacrylate (98%), *N*-(1-pyrene)maleimide, butyl acetate (99.7%) and aluminium oxide basic were purchased from Sigma Aldrich Fluka. All monomers were passed over basic aluminum oxide before use. 4,4′-Azobis(4-cyanovaleric acid) (>98%) (ABCVA), Span 80, Tween 80, sodium cyclopentadienide (2 M in THF), and ammonium chloride (>99.5%) were pur-

chased from Sigma and were used as received. Cyclohexane, hexane, tetrahydrofuran, ethanol, acetonitrile and hydrochloric acid were purchased from VWR. Solvents were used as received.

Preparation of PEG-*co*-GMA microgel

The PEG-*co*-GMA microgels were synthesized by suspension polymerization with ABCVA as an initiator in a 500 mL round bottom flask with temperature and stirring control. First, monomers ((PEGMA, M_n: 500 g mol^{-1}, 7 g, 0.014 mol), glycidyl methacrylate (GMA, 900 mg, 6.3 mmol), ABCVA (250 mg, 0.89 mmol), ethylene glycol dimethacrylate (EGDMA, 420 mg, 2.12 mmol)) (molar ratio 0.7/0.3/0.05/0.1) were dissolved in a mixture of 12 mL water/acetonitrile 5/1 (40% w/w) and the solution was transferred into a separated flask containing 200 mL of cyclohexane containing the surfactant (mixture of Span 80 and Tween 80 HLB: 5.9). The flask was degassed with N_2 for 30 min. Polymerization was carried out at 70 °C under stirring at 400 rpm for 6 h. The particle size is controlled by the stirring speed. Microgels were dried after washing and cleaning.

Preparation of Cp funtionalized PEG microgels

PEG microgels (3 g) were suspended in 200 mL of dry THF in a round bottom flask and cooled in an ice-salt bath to −10 °C. A solution of sodium cyclopentadienide in THF (2 M, 4.8 mL, 12 mmol) into 25 mL of dry THF was added dropwise to microgels. After 1 h, the ice-salt bath was removed and the mixture was lightly stirred for another 3 hours at ambient temperature. The reaction was quenched by pouring the reaction mixture into 200 mL of saturated NH_4Cl solution. Subsequently, the microgels were filtered off and washed successively by 200 mL of acetone, ethanol–water (1/1), 3% HCl in water, water, THF and hexane. Microgels were kept in ethanol for better storage.

Derivatization for fluorescence microscopy

Cp-PEG microgels (50 mg) and *N*-pyrene maleimide (20 mg, 68×10^{-3} mmol) were suspended in 2.5 mL of dry THF in a flask and were stirred for 4 hours at 40 °C. The microgels were washed thoroughly (3 × 25 mL of THF and 3 × 25 mL of ethanol) to remove the physically absorbed pyrene moiety.

UV quantitative study

A fresh stock solution of 4-phenyl-1,2,4-triazoline-3,5-dione (PTAD) (M_w: 175.14 g mol^{-1}, 4.35 mg into 5 mL, 0.497 M) in butyl acetate was used as titration species. A calibration curve was made using 5 different concentrations of PTAD solutions. The following titration procedure was used: 100 μL of a suspension of microgels were added into a vial with 2.4 mL of butyl acetate. A defined volume of PTAD stock solution (50 μL) was added into the vial and the mixture was stirred for 5 minutes. The solution was filtered on a micro-disk with a pore size diameter of 0.5 μm. The filtered solution was characterized by UV to determine the remaining PTAD after reaction with the cyclopentadienyl function onto the microgel surface.

DX microgel synthesis

200 μL of butyl acetate and 400 mg of a suspension of swollen microgels (12 g of swollen microgels + 3 mL of butyl acetate) were added into a small vial. To the resulting microgel suspension, 33 μL (82×10^{-9} mole) of a stock solution of MDI-TAD (4.5 mg into 5 mL) was added. The suspension was stirred to promote homogeneity in the vial until the gelation occurred.

Equipment

Mechanical characterization by dynamic rheology. Dynamic rheology measurements were performed using an Anton Paar Physica MCR 310 Rheometer in oscillatory mode with a temperature-controlled rheometer equipped with an environmental chamber. A 20 mm diameter plate geometry was used.

UV spectrometer. UV measurements were performed on a UV spectrometer Analytik-jena Specord 200.

Optical microscopy. Optical microscopy measurements were performed on an Olympus Optical microscope with a Canon camera.

Particles size measurements. Particle size measurements were performed on a Beckman Coulter LS 200 particles sizer.

Fluorescence microscopy. Microgels were observed in epifluorescence mode with an inverted Nikon Eclipse Ti-E motorized microscope (Nikon, Japan) equipped with ×10 Plan Apo (NA 1.45), ×40 Plan Apo (NA 1.45, oil immersion) and ×60 Plan Apo (NA 1.45, oil immersion) objectives, two lasers (Ar-ion 488 nm; HeNe, 543, 543 nm) and a modulable diode (408 nm). Epifluorescence images were captured with a Roper QuantEM:512SC EMCCD camera (Photometrics, Tucson, AZ) using NIS Elements AR (Nikon, Japan). To quantify the fluorescence signal, microgels were observed in epifluorescence under similar conditions (objective, light intensity, gain, and camera frequency). The microbead outline was automatically detected with the NIS element using a mask obtained from a thresholded fluorescence image. The microbead area, the raw integrated density and the mean gray value were obtained for each microbead. In addition, five random background regions were near each microbead to obtain a mean gray value of the fluorescent background. The corrected microgel fluorescence was calculated using the following relation: corrected microgel fluorescence = raw integrated density − (microgel section × mean fluorescence background).

SEM. DX microgel was imaged with a field emission gun scanning electron microscope (FEG-SEM Hitachi SU8020).

Abbreviations

W/O	Water in oil
TAD	Triazolinedione
Cp	Cyclopentadiene
GMA	Glycidyl methacrylate
EGDMA	Ethylene glycol dimethacrylate
HDA	Hetero-Diels alder
PEGMA	Polyethylene glycol methyl ether methacrylate
MDI-TAD	4,4′-(4,4′-Diphenylmethylene)-bis-(1,2,4-triazoline-3,5-dione)

MG	Microgel
ABCVA	4,4′-Azobis(4-cyanovaleric acid)
PTAD	4-Phenyl-1,2,4-triazoline-3,5-dione
G'	Storage modulus
G''	Loss modulus
THF	Tetrahydrofuran

Funding sources

Work in the author's laboratories has been funded by grants from Ghent and Mons University.

Acknowledgements

L. M., P. D. and F. D. P. acknowledge the Belgian Program on Interuniversity Attraction Poles initiated by the Belgian State, the Prime Minister's office (P7/05). CIRMAP is grateful to the "Belgian Federal Government Office Policy of Science (SSTC)" for general support in the frame of the PAI-7/05, the European Commission and the Wallonia Region (FEDER Program), and OPTI2MAT program of excellence. C. B.-K. acknowledges continued support from the Karlsruhe Institute of Technology (KIT) in the context of the Helmholtz BIFTM and STN programs.

Notes and references

1 J. A. Yang, J. Yeom, B. W. Hwang, A. S. Hoffman and S. K. Hahn, *Prog. Polym. Sci.*, 2014, **39**, 1973–1986.
2 D. Y. Ko, U. P. Shinde, B. Yeon and B. Jeong, *Prog. Polym. Sci.*, 2013, **38**, 672–701.
3 J. A. Burdick and G. D. Prestwich, *Adv. Mater.*, 2011, **23**, H41–H56.
4 C. T. Huynh, M. K. Nguyen and D. S. Lee, *Macromolecules*, 2011, **44**, 6629–6636.
5 E. K. Yetimoglu, M. V. Kahraman, G. Bayramoglu, O. Ercan and N. K. Apohan, *Radiat. Phys. Chem.*, 2009, **78**, 92–97.
6 J. L. Wang, J. Wei, S. Su, J. Qiu and S. Wang, *J. Mater. Sci.*, 2015, **50**, 5458–5465.
7 Z. Q. Ren, Y. Zhang, Y. Li, B. Xu and W. Liu, *J. Mater. Chem. B*, 2015, **3**, 6347–6354.
8 H. Park, E. K. Woo and K. Y. Lee, *J. Controlled Release*, 2014, **196**, 146–153.
9 J. Y. Sun, X. Zhao, W. R. K. Illeperuma, O. Chaudhuri, K. H. Oh, D. Mooney, J. Vlassak and Z. Suo, *Nature*, 2012, **489**, 133–136.
10 X. Hao, W. Zhou, R. Yao, Y. Xie, S. Rehman and H. A. Yang, *J. Mater. Chem. A*, 2013, **1**, 14612–14617.
11 Y. Chen, X. H. Pang and C. M. Dong, *Adv. Funct. Mater.*, 2010, **20**, 579–586.
12 J. Wang, Y. Xu, Y. Wang, J. Liu, J. Xu, L. Li, H. T. Nguyen, D. T. Pham, S. F. Lincoln and X. Guo, *RSC Adv.*, 2015, **5**, 46067–46073.
13 H. T. Cui, L. Cui, P. Zhang, Y. Huang, Y. Wei and X. Chen, *Macromol. Biosci.*, 2014, **14**, 440–450.
14 F. Li, J. He, M. Zhang, K. C. Tam and P. Ni, *RSC Adv.*, 2015, **5**, 54658–54666.
15 S. J. De Jong, B. Van Eerdenbrugh, C. F. Van Nostrum, J. J. Kettenes-Van den Bosch and W. E. Hennink, *J. Controlled Release*, 2001, **71**, 261–275.
16 J. Slager and A. J. Domb, *Adv. Drug Delivery Rev.*, 2003, **55**, 549–583.
17 C. Hiemstra, Z. Zhong, S. R. Van Tomme, M. J. Van Steenbergen, J. J. L. Jacobs, W. D. Otter, W. E. Hennink and J. Feijen, *J. Controlled Release*, 2007, **119**, 320–327.
18 A. P. Nowak, V. Breedveld, L. Pakstis, B. Ozbas, D. J. Pine, D. Pochan and T. J. Deming, *Nature*, 2002, **417**, 424–428.
19 C. C. Huang, S. Ravindran, Z. Yin and A. George, *Biomaterials*, 2014, **35**, 5316–5326.
20 R. L. Huang, W. Qi, R. Su and Z. He, *Soft Matter*, 2011, **7**, 6222–6230.
21 M. Kurecic, M. Sfiligoj-Smole and K. Stana-Kleinschek, *Mater. Tehnol.*, 2012, **46**, 87–91.
22 G. R. Bardajee, A. Pourjavadi, S. Ghavami, R. Soleyman and F. Jafarpour, *J. Photochem. Photobiol., B*, 2011, **102**, 232–240.
23 I. S. Kim, S. H. Kim and C. S. Cho, *Arch. Pharmacal Res.*, 1996, **19**, 18–22.
24 B. Q. Li, L. Wang, F. Xu, X. Gang, U. Demirci, D. Wei, Y. Li, Y. Feng, D. Jia and Y. Zhou, *Acta Biomater.*, 2015, **22**, 59–69.
25 Z. Q. Liu, Z. Wei, X. L. Zhu, G. Y. Huang, F. Xu, J. H. Yang, Y. Osada, M. Zrinyi, J. H. Li and Y. M. Chen, *Colloids Surf., B*, 2015, **128**, 140–148.
26 Y. X. Dong, Y. Qin, M. Dubaa, J. Killion, Y. Gao, T. Zhao, D. Zhou, D. Duscher, L. Geever, G. C. Gurtner and W. A. Wang, *Polym. Chem.*, 2015, **6**, 6182–6192.
27 K. S. Kim, S. J. Park, J. A. Yang, J. H. Jeon, S. H. Bhang, B. S. Kim and S. K. Hahn, *Acta Biomater.*, 2011, **7**, 666–674.
28 E. C. Cho, J. W. Kim, A. Fernandez-Nieves and D. A. Weitz, *Nano Lett.*, 2008, **8**, 168–172.
29 X. Q. Jia, Y. Yeo, R. J. Clifton, T. Jiao, D. S. Kohane, J. B. Kobler, S. Zeitels and R. Langer, *Biomacromolecules*, 2006, **7**, 3336–3344.
30 A. K. Jha, X. Xu, R. Duncan and X. Jia, *Biomaterials*, 2011, **32**, 4696–4704.
31 R. X. Liu, A. H. Milani, T. J. Freemont and B. R. Saunders, *Soft Matter*, 2011, **7**, 4696–4704.
32 E. C. Cho, J. W. Kim, D. C. Hyun, U. Jeong and D. A. Weitz, *Langmuir*, 2010, **26**, 3854–3859.
33 R. X. Liu, A. H. Milani, J. M. Saunders, T. J. Freemont and B. R. Saunders, *Soft Matter*, 2011, **7**, 9294–9306.
34 Z. B. Hu, X. Lu, J. Gao and C. Wang, *Adv. Mater.*, 2000, **13**, 2793–2801.
35 A. H. Milani, A. J. Freemont, J. A. Hoyland, D. J. Adlam and B. R. Saunders, *Biomacromolecules*, 2012, **13**, 2793–2801.
36 R. Liu, A. H. Milani, T. J. Freemont and B. R. Saunders, *Soft Matter*, 2011, **7**, 4696–4704.
37 S. Thaiboonrod, A. H. Milani and B. R. Saunders, *J. Mater. Chem. B*, 2014, **2**, 110–119.

38 A. H. Milani, J. Bramhill, A. J. Freemont and B. R. Saunders, *Soft Matter*, 2015, **11**, 2586–2595.
39 T. Lane, J. L. Holloway, J. M. Saunders, A. J. Freemont and B. R. Saunders, *Soft Matter*, 2013, **9**, 7934–7941.
40 N. Sahiner, A. K. Jha, D. Nguyen and X. Jia, *J. Biomater. Sci., Polym. Ed.*, 2008, **19**, 223–243.
41 T. Cai, G. Wang, S. Thomson, M. Marquez and Z. Hu, *Macromolecules*, 2009, **42**, 537–546.
42 A. K. Jha, R. A. Hule, T. Jiao, S. S. Teller, R. J. Clifton, R. L. Duncan, D. J. Pochan and X. Jia, *Maromolecules*, 2009, **42**, 537–546.
43 Z. X. Cui, A. H. Milani, P. J. Greensmith, J. Yan, D. J. Adlam, J. A. Hoyland, I. A. Kinloch, A. J. Freemont and B. R. Saunders, *Langmuir*, 2014, **30**, 13384–13393.
44 J. McParlane, D. Dupin, J. M. Saunders, S. Lally, S. P. Armes and B. R. Saunders, *Soft Matter*, 2012, **8**, 6239–6247.
45 S. R. Van Tomme, B. G. De Geest, K. Braeckmans, S. C. De Smedt, J. Siepmann, C. F. Van Nostrum and W. E. Hennink, *J. Controlled Release*, 2005, **110**, 67–78.
46 T. T. Gan, Y. J. Zhang and Y. Guan, *Biomacromolecules*, 2009, **10**, 1410–1415.
47 M. A. Tasdelen, *Polym. Chem.*, 2011, **2**, 2133–2145.
48 P. L. Golas and K. Matyjaszewski, *Chem. Soc. Rev.*, 2010, **39**, 1338–1354.
49 P. Espeel and F. E. Du Prez, *Macromolecules*, 2015, **48**(1), 2–14.
50 C. Barner-Kowollik, F. E. Du Prez, P. Espeel, C. J. Hawker, T. Junkers, H. Schlaad and W. Van Camp, *Angew. Chem., Int. Ed.*, 2011, **50**, 60–62.
51 J. O. Mueller, F. G. Schmidt, J. P. Blinco and C. Barner-Kowollik, *Angew. Chem., Int. Ed.*, 2015, **54**(35), 10284–10288.
52 R. Farley, S. Halacheva, J. Bramhill and B. R. Saunders, *Polym. Chem.*, 2015, **6**(13), 2512–2522.
53 S. Billiet, K. De Bruycker, F. Driessens, H. Goossens, V. Van Speybroec, J. M. Winne and F. E. Du Prez, *Nat. Chem.*, 2014, **6**, 815–821.
54 Z. K. Wang, L. Yuan, N. M. Trenor, L. Vlaminck, S. Billiet, A. Sarkar, F. E. Du Prez, M. Stefik and C. B. Tang, *Green Chem.*, 2015, **17**, 3806–3818.
55 K. De Bruycker, S. Billiet, H. A. Houck, S. Chattopadhyay, J. M. Winne and F. E. Du Prez, *Chem. Rev.*, 2016, **116**, 3919–3974.
56 O. Turunc, S. Billiet, K. De Bruycker, S. Ouardad, J. M. Winne and F. E. Du Prez, *Eur. Polym. J.*, 2015, **65**, 286–297.
57 J. P. Blinco, V. Trouillet, M. Bruns, P. Gerstel, H. Gliemann and C. Barner-Kowollik, *Adv. Mater.*, 2011, **23**, 4435–4439.
58 M. Kaupp, A. P. Vogt, J. C. Natterodt, V. Trouillet, T. Gruendling, T. Hofe, L. Barner and C. Barner-kowollik, *Polym. Chem.*, 2012, **3**, 2605–2614.
59 B. Falk and J. V. Crivello, *J. Appl. Polym. Sci.*, 2005, **97**(4), 1574–1585.
60 A. J. Inglis, M. H. Stenzel and C. Barner-Kowollik, *Macromol. Rapid Commun.*, 2009, **30**, 1792–1798.
61 M. Glassner, G. Delaittre, M. Kaupp, J. Blinco and C. Barner-Kowollik, *J. Am. Chem. Soc.*, 2012, **134**, 7274–7277.
62 F. Chambon and H. H. Winter, *J. Rheol.*, 1987, **31**, 683–697.
63 R. Liu, A. H. Milani, J. M. Saunders, T. J. Freemont and B. R. Saunders, *Soft Matter*, 2011, **7**, 9297–9306.

